Neurobiology of Aging 36 (2015) 1496–1504

Contents lists available at ScienceDirect

Neurobiology of Aging

journal homepage: www.elsevier.com/locate/neuaging

Sustained high levels of neuroprotective, high molecular weight, phosphorylated tau in the longest-lived rodent

Miranda E. Orr, Valentina R. Garbarino, Angelica Salinas, Rochelle Buffenstein*

Department of Physiology and The Barshop Institute for Longevity and Aging Studies, University of Texas Health Science Center at San Antonio, San Antonio, TX, USA

ARTICLE INFO

Article history:
Received 23 June 2014
Received in revised form 24 November 2014
Accepted 4 December 2014
Available online 12 December 2014

Keywords:
Tau
Phosphorylation
Alzheimer's disease
Naked mole-rat
Aging
Animal model

ABSTRACT

Tau protein is primarily expressed in neuronal axons and modulates microtubule stability. Tau phosphorylation, aggregation, and subcellular mislocalization coincide with neurodegeneration in numerous diseases, including Alzheimer's disease (AD). During AD pathogenesis, tau misprocessing accompanies Aß accumulation; however, AD animal models, despite elevated Aß, fail to develop tauopathy. To assess whether lack of tau pathology is linked to short life span common to most AD models, we examined tau processing in extraordinarily long-lived, mouse-sized naked mole-rats (NMRs; approximately 32 years), which express appreciable levels of Aß throughout life. We found that NMRs, like other mammals, display highest tau phosphorylation during brain development. Although tau phosphorylation decreases with aging, unexpectedly adult NMRs have higher levels than transgenic mice overexpressing mutant human tau. However, in sharp contrast with the somatodendritic accumulation of misprocessed tau in the transgenic mice, NMRs maintain axonal tau localization. Intriguingly, the adult NMR tau protein is 88 kDa, much larger than 45–68 kDa tau expressed in other mammals. We propose that this 88 kDa tau protein may offer exceptional microtubule stability and neuroprotection against lifelong, elevated Aß.

1. Introduction

The microtubule-associated protein tau regulates several distinct neuronal processes including microtubule nucleation, polymerization, polarity, dynamics, spacing, and bundling. Tau's functional importance becomes evident in patients with microdeletions in the coding gene, microtubule-associated protein tau (*MAPT*). Although exceedingly rare, these mutations result in mental retardation and craniofacial abnormalities (Rovelet-Lecrux and Campion, 2012). Correspondingly, mice homozygous for *Mapt* deletion display long term-potentiation impairments resulting in cognitive deficits (Ahmed et al., 2014). Far more frequently, tau negative regulation occurs through posttranslational phosphorylation (Lindwall and Cole, 1984), and tau misprocessing, initiated primarily through hyperphosphorylation, coincides with neurodegeneration in a variety of disorders (e.g., Pick disease, argyrophilic grain disease, progressive supranuclear palsy, frontotemporal dementia, and chronic traumatic encephalopathy as well as Alzheimer's disease [AD]) (Spillantini and Goedert, 2013). Several studies have revealed exacerbated pathology in animal models upon genetically ablating *Mapt* including enhanced tauopathy (Ando et al., 2011), lysosomal dysfunction (Pacheco et al., 2009), parkinsonism (Lei et al., 2012) as well as Aß-associated axonal degeneration (Dawson et al., 2010) underscoring the importance of functional tau during situations of neurotoxic stress.

The vast majority of patients afflicted with tauopathies develop the diseases sporadically with age being the greatest risk factor. Incongruously, the most common animal models for these diseases are short-lived mice that do not naturally develop tauopathy, possibly because of their short life span. To overcome this shortcoming, induction of pathology is accomplished through genetic overexpression of mutant human gene variants. Fully penetrant AD-inducing mutations, accounting for <2% of all AD cases, occur in genes encoding proteins responsible for the accumulation of toxic, aggregation prone $Aß_{1-42}$. The concomitant misprocessing of tau, cognitive decline, behavioral changes, neuronal loss, and brain atrophy suggests that Aß, alone, may drive AD. Discovery of these familial AD mutations engendered the "Aß hypothesis" (Hardy and Higgins, 1992) that posits Aß accumulation is necessary and sufficient to drive AD pathogenesis and tauopathy. Many AD models expressing elevated Aß display cognitive impairments but do not develop appreciable tau pathology unless multiple transgenes (e.g.,

*Corresponding author at: Department of Physiology and The Barshop Institute for Longevity and Aging Studies, University of Texas Health Science Center at San Antonio, 15355 Lambda Drive, San Antonio, TX 78245, USA. Tel.: +1 210 562 5062; fax: 210 5625028.
E-mail address: buffenstein@uthscsa.edu (R. Buffenstein).

0197-4580/$ – see front matter © 2015 Elsevier Inc. All rights reserved.
http://dx.doi.org/10.1016/j.neurobiolaging.2014.12.004

mutant human tau, (Oddo et al., 2003)) are also expressed and neurodegeneration seldom occurs (Wirths and Bayer, 2010). Strikingly, despite successful pharmacologic amelioration of AD pathology and attenuation of cognitive decline over 300 times in such animal models, none of these promising preclinical findings have translated into effective and safe human therapies (Zahs and Ashe, 2010). The reasons, although not entirely clear, may reflect the modeling of the extremely rare heritable diseases in short-lived mammals, rather than addressing the more common sporadic nature of tauopathy and the use of model systems with life spans long enough to track pathogenesis.

Recently, we discovered naturally expressed, high levels of Aß in the brains of the naked mole-rat (NMR, *Heterocephalus glaber*), the longest-lived rodent known (Edrey et al., 2013). These mouse-sized rodents defy maximum life span predictions by living approximately 5 times longer than expected based on their body size and approximately 8 times longer than similar-sized mice. With a maximum life span of >30 years, they offer an exceptional perspective to investigate age-associated diseases. Many NMRs express higher brain Aß levels than do 3xTg-AD mice (Edrey et al., 2013), a well-characterized mouse model of AD pathology genetically manipulated to express high levels of this toxic peptide (Oddo et al., 2003). The NMR Aß peptide differs from that of human Aß by one amino acid, but both human and NMR Aß exert similar neurotoxicity to mouse cortical neurons in vitro (Edrey et al., 2013). NMRs, however, do not develop manifest plaques and seemingly maintain neuronal integrity. We wondered whether tau metabolism remained properly regulated despite >30 years of high levels of Aß peptide. Specifically, we investigated whether NMR tau protein was similar to human tau (e.g., sequence, size, expression, and phosphorylation), how it changed with age, and whether lifelong elevated levels of Aß altered tau misprocessing in NMRs. We assessed levels of total tau, phosphorylated tau, and known tau kinases throughout the NMR 30-year life span and compared adult brain histology with that of well-characterized 3xTg-AD mice.

2. Methods

2.1. Animals

Animal procedures were carried out in adherence to NIH, Federal, State, and Institutional guidelines at University of Texas Health Science Center San Antonio (University of Texas Health Science Center at San Antonio UTHSCSA; protocol #07123).

2.2. Tissue collection

Brains from 38 NMRs (<1 year) and 24 (>1 year) were collected. Animals were anesthetized by isoflurane inhalation then transcardially perfused with ice-cold phosphate-buffered saline (PBS), pH 7.4. Brains were immediately harvested, weighed, and sagitally bisected. One hemibrain was drop fixed in 10% zinc formalin for 48 hours, then transferred to PBS containing 0.02% sodium azide, and stored at 4 °C until further histologic processing. The other hemibrain was snap frozen in liquid nitrogen and stored at −80 °C for future biochemical analyses.

2.3. Tissue homogenization

For biochemistry, frozen hemibrains (minus cerebellum and brain stem) were slightly thawed on ice and mechanically homogenized with dounce and pestle in ice-cold buffer H (10 mM Tris HCl pH 7.4, 1 mM EGTA, 0.8 M NaCl, 10% sucrose) containing complete protease inhibitor (Roche, Basel, Switzerland) with or without phosphatase inhibitors (Invitrogen, Carlsbad, CA). Brain homogenates were centrifuged 14,000 rpm for 20 minutes at 4 °C. The supernatant was used for all further capillary electrophoresis. Protein concentration was determined using BCA assay (Pierce, Rockford, IL).

2.4. Capillary electrophoresis immunoassay

Capillary electrophoresis immunoblotting, or Simple Western analyses, were performed using the Simon and Wes platforms for tau and tau kinase levels, respectively, according to the manufacturer's protocol (ProteinSimple, Santa Clara, CA). This state of the art technology is considered more sensitive and quantitative than traditional Western blot immunoblotting, generating highly reproducible electropherograms with precise peaks and facilitating accurate molecular weight assessments (Creamer et al., 2014; Nguyen et al., 2011). In brief, brain homogenate was diluted to 6 μg (for Simon) or 1 μg (for Wes) in sample buffer and added to a master mix containing dithiothreitol and fluorescent molecular weight marker then heated at 95 °C for 5 minutes. The chemiluminescent substrate, HRP-conjugated secondary antibody, primary antibody, blocking reagent, samples, and separation and stacking matrices were dispensed into a 384-well plate. After plate loading, the separation electrophoresis and immunodetection steps took place in the capillary system and were fully automated. Simple Western analysis is carried out at room temperature and instrument default settings were used. Primary antibodies used the following: rabbit anti-total and phospho-GSK3ß Ser^{9}, total and phospho-ERK1/2 $Thr^{202/204}$ and $Thr1^{85/187}$, Cdk5, p35, and mouse anti-Tau46 (1:50) and mouse anti-GAPDH (1:100) (Cell Signaling, Danvers, MA). Dilutions of anti-tau antibodies are as follows: Tau1 (1:100); RD3, RD4, and Tau5 (1:50) (Millipore, Billerica, MA); mouse anti-CP13 and PHF1 (1:10) (generous gifts from Peter Davies); mouse anti-HT7 (1:50) (Pierce). Recombinant human tau was purchased (rPeptide, Bogart, GA). All antibodies were diluted with antibody diluent (ProteinSimple). The digital image was analyzed with Compass software (ProteinSimple v2.5), and the quantified data of the detected protein were reported as molecular weight. Protein densitometry was calculated by dividing the area under the curve of each protein of interest by area under the curve of GAPDH loading control.

2.5. Phosphatase assay

For removing posttranslational phosphorylation, brain homogenates were suspended in 0.8 μg/μL of NEBuffer 3 and incubated with 20U/μL of calf intestinal phosphatase (CIP) (New England Biolabs, Ipswich, MA) for 60 minutes at 37 °C. CIP-treated samples were compared with samples incubated in NEBuffer 3 without CIP.

2.6. Immunohistochemistry

Zinc formalin-fixed tissues were sectioned (30 μm thick) using a sliding vibratome and stored in 0.02% sodium azide in PBS until immunostaining was conducted. The endogenous peroxidase activity was quenched with 3% H_2O_2 in 10% methanol for 30 minutes. Tissue was incubated overnight at 4 °C with corresponding primary antibody. Sections were washed in tris-buffered saline and incubated in biotinylated secondary antibody for 1 hour at 20 °C. Sections were developed with diaminobenzidine substrate using the avidin-biotin horseradish peroxidase system (Vector Labs, Burlingame, CA, USA). Primary antibodies: HT7 (1:3000) and CP13 (1:2000). Images were obtained with a Zeiss camera. For each antibody, all tissues were immunostained simultaneously to eliminate batch-to-batch variability in antibody concentrations, incubation times, or chromogen exposure. Similarly, all images were acquired using identical settings to prevent light, exposure, or other subtle microscopy differences. As such, relative differences in immunostaining at the various ages can be compared with confidence.

2.7. Statistics

All data were analyzed using GraphPad Prism version 6.0c for Mac OS X, GraphPad Software, San Diego CA, USA, www.graphpad.com/. Data were analyzed by 1-way analysis of variance.

2.8. Sequence alignment

Known human tau protein sequences and predicted NMRs were acquired from NCBI. Clustal Omega was used for sequence alignment.

3. Results

3.1. NMR tau protein sequence is highly similar to human tau

Human *MAPT* is a single copy gene that undergoes alternative splicing to generate several unique splice variants; six splice variants are expressed in the adult brain (Goedert et al., 1989a,b,). Although no information regarding NMR tau protein is available, the NMR genome has been sequenced (Kim et al., 2011), and predicted protein sequences are accessible through NCBI and the Naked Mole-Rat Genome Resource 2014 (http://naked-mole-rat.org). The NMR brain, like human brain, generates 2 *Mapt* transcripts, 2 and 6 kb, with several projected tau proteins (Goedert et al., 1989a,b; Kim et al., 2011; http://naked-mole-rat.org/). NMR *Mapt* isoform X2 with a predicted amino acid length of 446 is most similar in identity and length to the longest human brain tau splice variant, 441 amino acid isoform 4R2N. Protein alignment comparison illustrates high homology between species (95% identical) and 100% identity at the functional microtubule-binding domain (Fig. 1). Additionally, the comparison indicates high conservation of NMR tau at antibody epitopes commonly used to study human tau including total tau antibodies: HT7, Tau5, Tau46; microtubule-binding domains: RD3 and RD4; phospho-tau: CP13 and PHF1; and non-phospho-tau: Tau1. Immunoblotting with these antibodies revealed that NMR tau protein is highly immunoreactive to antibodies against the functional microtubule–binding domains, middle, and C-terminus as indicated by strong immunoreactivity to RD3, RD4, HT7, Tau5, and Tau46, respectively. Strikingly, the NMR protein is dramatically larger than tau expressed in adult wild-type mice or transgenic human tau expressing mice (Fig. 2A). The prominent adult NMR tau protein is approximately 88 kDa, which is much larger than the heaviest human tau protein band migrating at approximately 72 kDa (Fig. 2A).

3.2. NMR tau undergoes a progressive increase in molecular weight during development

Because differential tau processing occurs between development and adulthood in other mammals (Goedert et al., 1989b; Himmler et al., 1989), we assessed the developmental and aging profile of NMR total tau using capillary electrophoresis (CE). This highly reproducible quantitative technology facilitates the precise discernment of protein molecular weight as well as protein levels in myriad cell lines and tissues including brain (Beccano-Kelley et al., 2014; Creamer et al., 2014; Nguyen et al., 2011). At birth, NMR brain tau appears as doublet bands migrating at 62 and 72 kDa. These proteins persist through 2 weeks of age with the 72 kDa protein becoming more abundant. Around 3 weeks of age, the lower 62 kDa band disappears, and the 72 kDa band becomes the prominent tau protein expressed. At 3 months of age, expression of higher molecular weight tau protein begins to occur with the emergence of an 88 kDa band and by 1 year of age this becomes the predominant tau protein (Fig. 2B and C).

3.2.1. NMR tau expression decreases with age

To better understand how levels of total tau were affected by age and the contribution of phosphorylation to the molecular weight shift observed, we examined levels of total and phosphorylated tau throughout the NMR life span. Levels of total tau are highest during postnatal development and then significantly decrease by 1 month of age (analysis of variance [ANOVA], $p = 0.0184$) where a constant expression level is maintained for the next 2 years of life. A significant decrease in total tau expression occurs in the 7- to 10-year-old cohort (ANOVA, $p = 0.0033$), and this level is maintained through the rest of mid-late adulthood (Fig. 3A and B). Immunohistochemical (IHC) analysis of cortical brain tissue compliments the CE results whereby high protein expression occurs through 3 weeks of age and lower total tau levels are expressed in the adult brain (Fig. 3C).

3.2.2. Tau phosphorylation levels decrease with age in cortical and hippocampal brain tissue

During development the nervous system requires a dynamic cytoskeleton permissive to axonal migration, neurite outgrowth, and

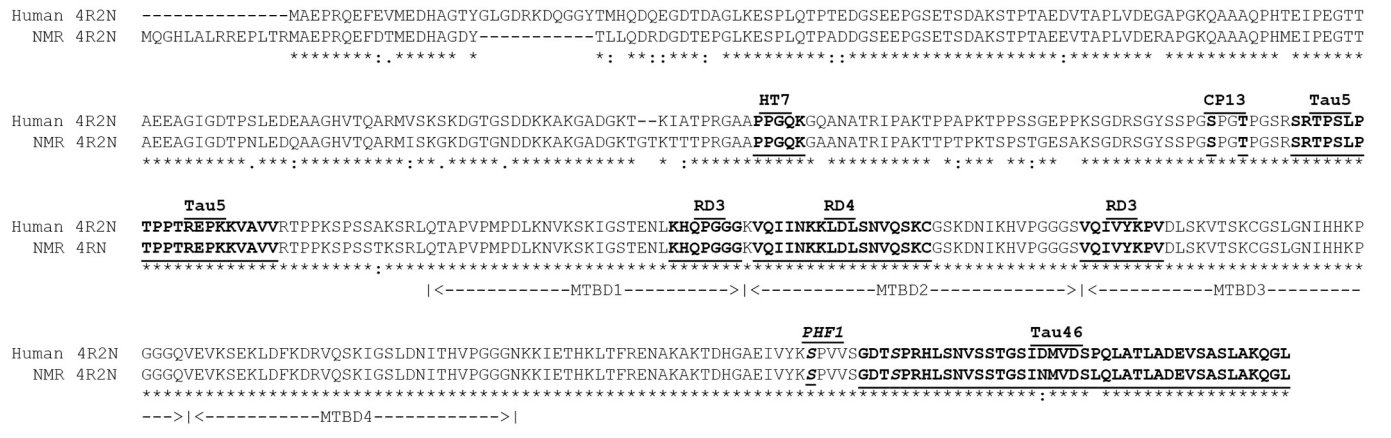

Fig. 1. Predicted naked mole-rat tau amino acid sequence is highly similar to human tau. The longest human brain tau protein splice variant (4R2N) aligned to a putative naked mole-rat tau protein indicates the highest conservation at the carboxy-terminus with 100% identity at the functional microtubule-binding domain. Antibody epitopes used in this study are indicated by underline and bold typeface. HT7, Tau46 and Tau5 indicate total tau antibodies; CP13 and Tau1 recognize tau phosphorylated, or not, respectively, at Ser^{202}/Thr^{205}; PHF1 recognizes tau phosphorylated at $Ser^{396/404}$. Asterisk (*) indicates a fully conserved residue; colon (:) indicates conservation between groups of strongly similar properties; period (.) indicates conservation between groups of weakly similar properties. Amino acid numbering derived from human 4R2N splice variant. Abbreviation: MTBD, microtubule-binding domain.

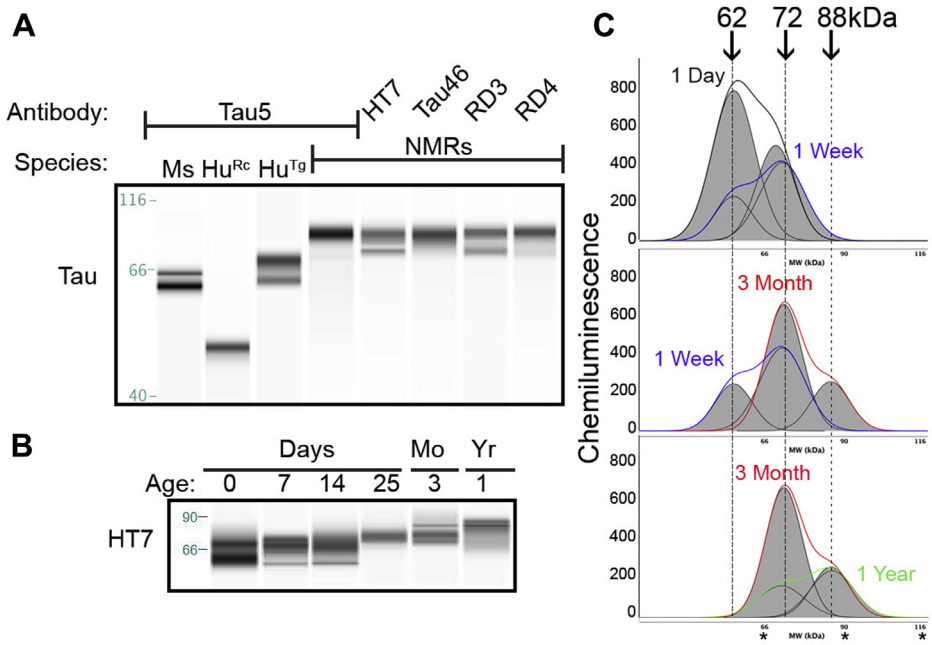

Fig. 2. Immunoblotting naked mole-rat (NMR) brain homogenates using capillary electrophoresis with anti-human tau antibodies indicates high protein sequence homology and a unique NMR-expressed tau protein. (A) NMR tau is immunoreactive to many well-characterized anti-tau antibodies. Based on human tau 4R2N sequence, Tau5 recognizes tau amino acids 210–229, a region immediately upstream of the microtubule-binding domains; HT7 recognizes tau amino acids 159–163 within the proline-rich domain; and Tau46 recognizes the far carboxy-terminal residues 401–441. RD3 and RD4 recognize tau proteins lacking (RD3) or expressing (RD4) microtubule-binding domain 2. NMR tau is immunoreactive to all antibodies and appears as a much larger protein with slower electrophoretic mobility than either mouse (Ms) or human (Hu) tau. (B) Artificial immunoblots produced by capillary electrophoresis clearly illustrate that NMR tau undergoes a progressive shift in molecular weight during development. (C) The capillary electrophoresis electropherograms allow the acute discernment of distinct protein bands, which then generates the artificial blot shown in B. Electropherograms indicate that neonatal NMR tau consists of 2 distinct bands: a prominent 62 kDa band and a minor 72 kDa band. During the first week of development, 72 kDa tau expression increases to levels higher than 62 kDa tau. By 3 months of age, 72 kDa tau is heavily expressed and the emergence of a higher 88 kDa band appears. By 1 year of age the high molecular weight 88 kDa tau protein becomes the prominent tau protein with lower levels of 72 kDa band remaining. Asterisks on electropherograms indicate 66, 90, and 116 kDa, respectively. Abbreviations: Hu^{Rc}, recombinant human tau 4R2N; Hu^{Tg}, transgenic mouse expressing wild type human tau (Andorfer et al., 2003); hTau, human tau; Mo, months; Ms, mouse; Yr, year. (For interpretation of the references to color in this Figure, the reader is referred to the Web version of this article.)

extension. To facilitate this fluid cytoskeleton, tau protein is heavily phosphorylated allowing for rapid dissociation and microtubule disassembly (Brion et al., 1993). Human fetal tau contains 7 moles of phosphate per mole of protein, which greatly contrasts to the healthy adult brain with only 1–3 moles of phosphate per mole of tau (Kenessey and Yen, 1993). To determine whether NMRs express measurable levels of phosphorylated tau, we conducted CE and IHC on NMR brains across their 30-year life span. The amount of NMR tau phosphorylated at $Ser^{396/404}$, epitopes phosphorylated during development, and AD pathogenesis was determined by probing samples with the PHF1 antibody. NMR brains express high amounts of PHF1 immunoreactive protein that significantly depends on age (Fig. 4. ANOVA, $p < 0.0001$). The highest level of phospho-tau protein expression occurs during early development. Neonate brains contain 42.9% more phospho-tau than 3-month-old NMRs (ANOVA, $p = 0.0003$). PHF1 immunoreactivity drops significantly, nearly half (44.9%), again by 6 months of age (ANOVA, $p = 0.0152$). Phosphorylated-tau levels remain constant throughout the remainder of the NMR life span suggesting this age, 6 months, may represent a transition to a mature adult brain (Fig. 4A and B).

To better determine the contribution of tau phosphorylation on the developmental molecular weight shift, we treated brain homogenates with calf alkaline phosphatase (CIP) to promote dephosphorylation. We compared 2-week-old and 2-year-old NMRs because tau protein from these ages greatly differs in size and appropriately represent development and adulthood, respectively (Fig. 2B). We compared untreated and CIP treated brain homogenates to recombinant human tau 4R2N. A shift in total tau molecular weight occurs with phosphatase treatment (Fig. 4C, HT7) in both 2-week-old and 2-year-old samples, suggesting that tau phosphorylation contributes to molecular weight in both ages and corroborates the PHF1 phosphorylation data (Fig. 4A). We used an antibody specific to non-phosphorylated tau, Tau1, as an additional control to ensure efficacy of the phosphatase treatment. Indeed, Tau1 immunoreactivity dramatically increased on phosphatase treatment and coincided with the absence of PHF1 immunoreactivity. Notably, 2-year-old NMR tau is larger than 2-week-old NMR tau even after dephosphorylation indicating the difference in molecular weight is not entirely because of phosphorylation (Fig. 4C). Furthermore, dephosphorylated NMR tau is much larger than recombinant human tau 4R2N, indicating molecular weight differences between species extend beyond posttranslational phosphorylation (Fig. 4C).

To evaluate the distribution of tau phosphorylation throughout the NMR brain, we conducted IHC with the phospho-specific antibody, CP13, which recognizes tau phosphorylated at Ser^{202}/Thr^{205}, an epitope phosphorylated during development and also during early stages of early AD pathogenesis. As seen with CE, the highest levels of phosphorylation occur early in development in both the cortex as well as hippocampal CA1 (Fig. 4D). Additionally, a dramatic decrease occurs around 6 months of age, and this lower level of phosphorylation is maintained throughout the next decades of life similar to results with total tau and PHF1 tau antibodies.

3.3. Protein levels of tau kinase increase with age

During brain development, axons actively migrate to seek out and build appropriate neuronal circuits; this requires a dynamic microtubule cytoskeleton with phospho-tau mechanistically achieved by active tau kinases. To evaluate tau kinase expression level

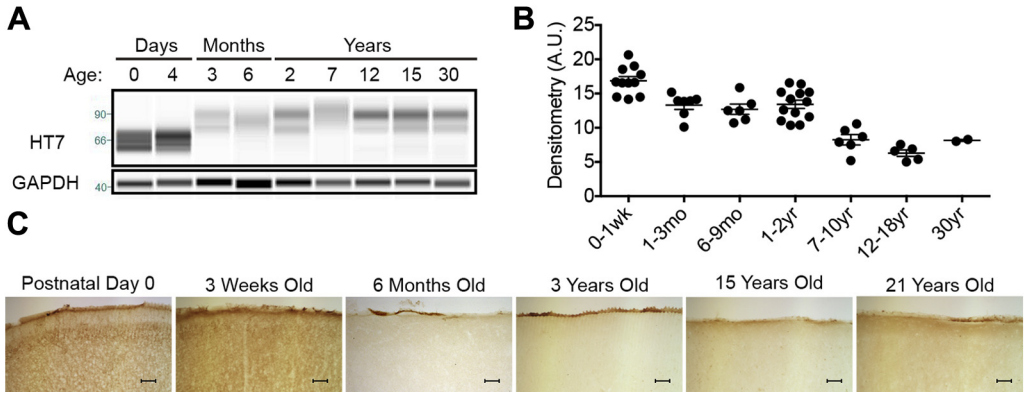

Fig. 3. The level of total tau expression significantly decreases during the naked mole-rat's long life span. (A) Artificial immunoblots produced by capillary electrophoresis graphically display total tau levels during the 30-year NMR life span. (B) Densitometric normalization of the electropherograms illustrate that total tau expression significantly decreases with NMR age (ANOVA, $p < 0.0001$). A significant change occurs throughout development with the highest expression during the first weeks of life and by 6 months of age, total tau levels have significantly decreased (20.5% decrease; ANOVA, $p = 0.0496$) The level of total tau is well maintained from 6 months through early adulthood and then significantly decreases in the 7- to 10-year-old cohort (ANOVA, $p = 0.0133$) and remains at this level throughout the remainder of the naked mole-rat life span. (C) Histologic assessment of brain tau expression coincided with the capillary electrophoresis data revealing the highest expression during the first weeks of life, a notable decrease at 6 months of age and then similar expression throughout the next 2 decades of life. Scale bar: 100 μm. Abbreviation: ANOVA, analysis of variance. (For interpretation of the references to color in this Figure, the reader is referred to the Web version of this article.)

and regulation throughout development and adulthood, we determined the relative amounts of total GSK3ß, Cdk5, and ERK1/2 tau kinases. Each of these well-characterized kinases is recognized for their importance in physiological brain development as well as pathogenic neurodegenerative cascades. Furthermore, we immunoprobed for kinase regulators to gain mechanistic insight into kinase activity. Specifically, we evaluated levels of Cdk5 co-activator, p35, and regulatory phosphorylation of GSK3ß and ERK1/2. We found strong antibody immunoreactivity to total and phosphorylated kinases in NMR brains at all ages; the total and phospho-ERK1/2 antibodies were far more immunoreactive to total and phospho-ERK2 than ERK1. NMRs may preferentially use ERK2, and from here forward we discuss ERK2 only. Levels of total Cdk5, p35, and ERK2 did not differ with age. However, total GSK3ß expression levels significantly decreased when animals reached sexual maturity (6–9 months) (Fig. 5A and C). Notably, this

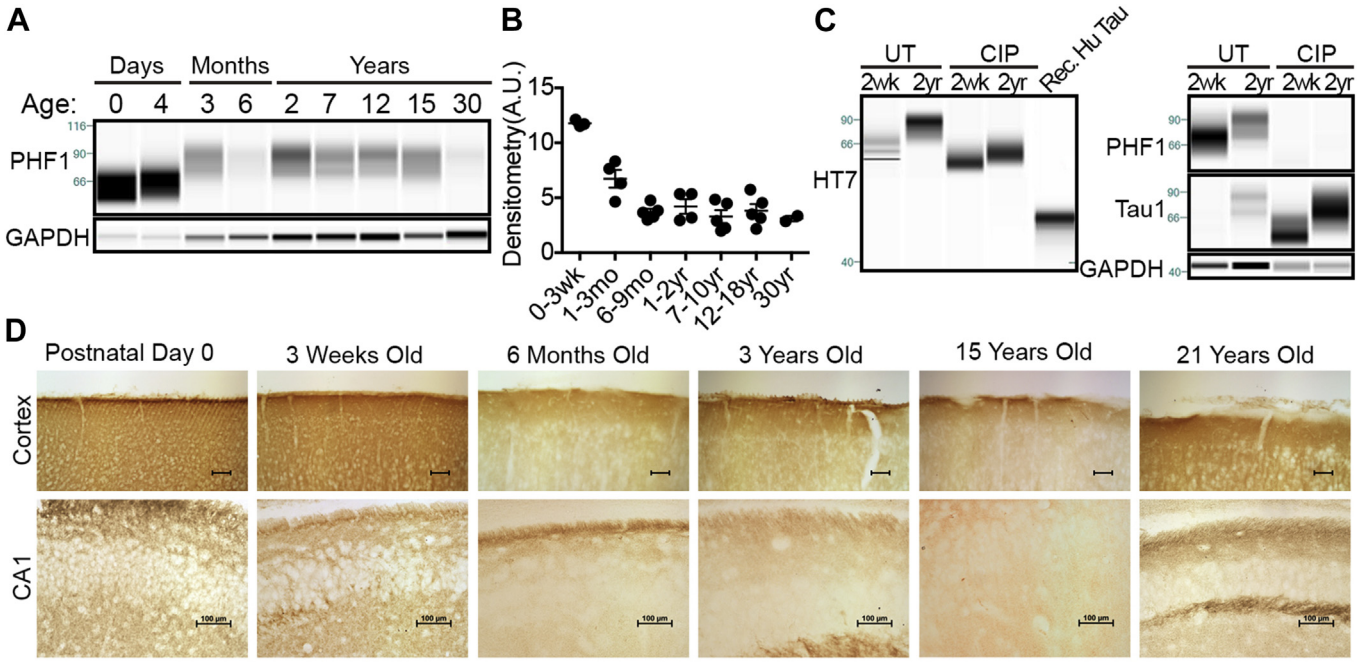

Fig. 4. Phosphorylation partly contributes to the age-associated increase in naked mole-rat (NMR) tau molecular weight. (A) Adult and neonatal NMR tau is heavily phosphorylated at AD-associated epitope $Ser^{396/404}$. NMR tau is most heavily phosphorylated during development and significantly changes with age (ANOVA, $p < 0.0001$). (B) Densitometric analysis indicates that PHF1 immunoreactivity decreases 32% after first week of life (ANOVA, $p = 0.0159$) and then drops significantly again between 3 and 6 months (52% decrease; ANOVA, $p = 0.0081$) where levels then remain statistically similar throughout the rest of life. (C) Protein dephosphorylation with calf intestinal phosphatase (CIP) indicates that phosphorylation contributes to a large portion of the total molecular weight. Although untreated tau from 2-week-old animals migrates as a 62, 66, 72 kDa triplet, dephosphorylated tau migrates as a single dense tau species approximately 60 kDa immunoreactive to Tau1 but not PHF1. Recombinant human 4R2N tau migrates at 49 kDa. Untreated 2-year-old animals express a prominent 88 kDa tau band, whereas dephosphorylation reveals a strong approximately 66 kDa tau species immunoreactive to Tau1 but not PHF1. (D) In accord with capillary electrophoresis data, immunohistochemistry with phospho-Ser^{202}/Thr^{205} tau antibody, CP13, shows the highest levels of phospho-tau in development, a dramatic decrease at 6 months and with maintained levels throughout life in the cortex and hippocampal CA1. Scale bars: 100 μm. Abbreviations: AD, Alzheimer's disease; ANOVA, analysis of variance. (For interpretation of the references to color in this Figure, the reader is referred to the Web version of this article.)

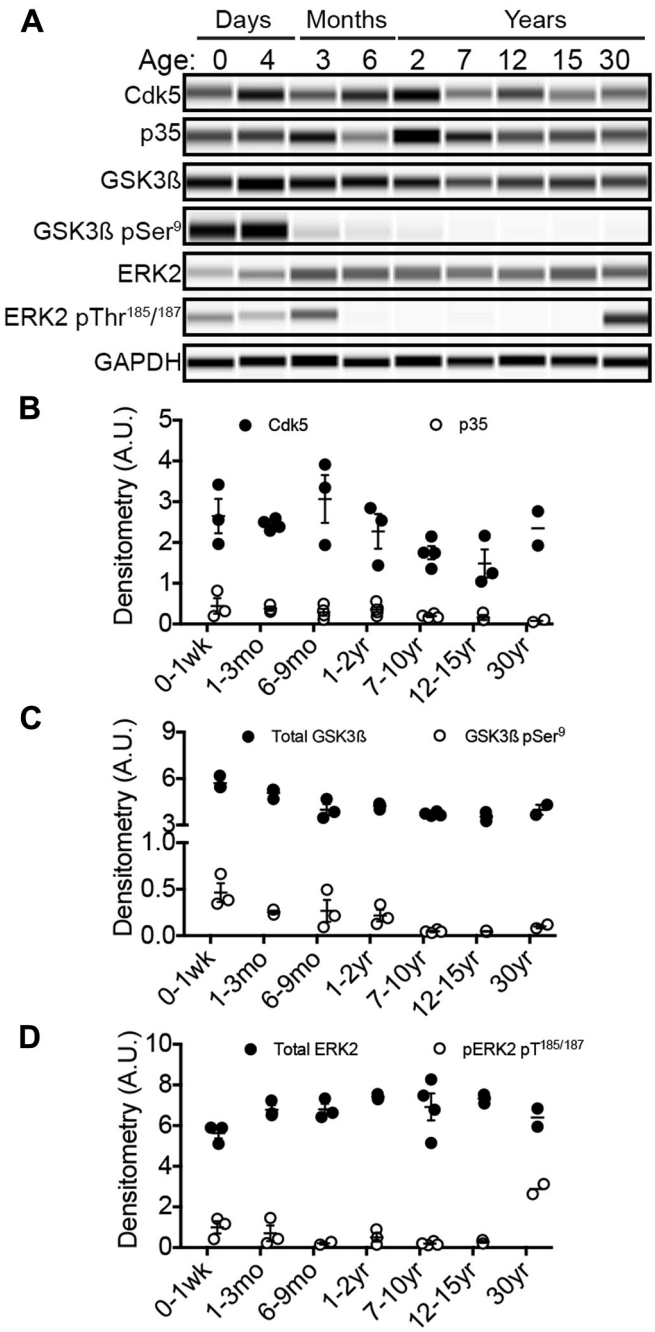

Fig. 5. Alzheimer's disease-associated tau kinase protein levels remain in a narrow range throughout naked mole-rat life. (A) Artificial blots produced by capillary electrophoresis using antibodies against total tau kinases and their corresponding regulators. Shown are the representative blots for Cdk5 and its co-activator, p35; total GSK3ß and inhibitory phosphorylation at residue Ser^{9}; total ERK2 and its activating phosphorylation at $Thr^{185/187}$ and corresponding GAPDH loading control. (B) Densitometry of Cdk5 and co-activator, p35, indicates stable expression throughout life. (C) Levels of GSK3ß significantly decrease during naked mole-rat life span (ANOVA, $p < 0.0001$). Specifically, GSK3ß is 30% higher during early neonatal development than in animals that have reached sexual maturity at 6–9 months (ANOVA, $p = 0.0008$); this adult level is maintained throughout life. Inhibitory phosphorylation at Ser^{9} significantly decreases throughout life span (ANOVA, $p = 0.0093$) whereby higher regulatory phosphorylation coincides with early neonatal development (0–1 week) than in the mature adults: 7- to 10-year olds (ANOVA, $p = 0.0087$), 12- to15-year olds (ANOVA, $p = 0.0209$). (D) Total ERK2 levels remain stable throughout life; activating phosphorylation only differs in the oldest 30-year-old cohort (ANOVA, $p < 0.0001$). Abbreviation: ANOVA, analysis of variance.

decrease in total GSK3ß level correlates well with the decrease in total and phospho-tau, indicating an important milestone in brain maturation for NMRs (Figs. 3 and 4). Levels of regulatory GSK3ß phosphorylation at Ser^{9} did not decrease significantly until mature adulthood (7 years old and beyond), which corresponds with the second major decline in total tau expression (Fig. 3). Interestingly, based on body size, NMRs have a predicted life span of 7–8 years. The significant decrease in total tau expression and regulatory kinase activity may indicate another critical stage in NMR brain development, maintenance, or maturity that we are continuing to explore. Levels of activated ERK2 phosphorylated at $Thr^{187/189}$ do not significantly differ with age except for in the oldest 30-year-old cohort (Fig. 5). Thirty-year-old NMRs are comparable with supercentenarian humans; although high ERK2 activation did not correlate with elevated phosphorylated tau in these animals, it may have implications in healthy brain aging and is worth exploring.

3.4. NMRs express significantly more total tau and phospho-tau than 3xTg-AD mice

Previously, we found that NMRs express higher levels of Aß than 3xTg-AD mice. To gain better perspective into the level of total and phospho-tau expression of NMRs, we directly compared them with 3xTg-AD mice. We found that young adult (2–7 years old) NMRs expressed approximately 4× more total tau and phospho-tau than 15-month-old 3xTg-AD mice with manifest pathology (Fig. 6A and B; unpaired *t* test, $p < 0.0001$ and $p = 0.0025$, respectively). Transgenic mutant human tau_{P301L} expressed by 3xTg-AD mice becomes hyperphosphorylated and mislocalizes from the axon to the somatodendritic compartment. However, despite higher expression levels of total tau, NMR tau remains appropriately localized in the axon as evidenced by strong immunoreactivity in mossy fibers indicating maintenance of physiological function (Fig. 6C).

4. Discussion

Tau misprocessing occurs early in disease pathogenesis in numerous neurodegenerative tauopathies. In the most prevalent of these, AD, Aß accrual has been hypothesized to drive tau pathology and downstream neurodegeneration (Hardy and Higgins, 1992). Interestingly, however, neurofibrillary tangles, comprised of hyperphosphorylated tau (phospho-tau), better correlate with AD severity (e.g., cognitive decline, behavioral changes, neuronal loss, and brain atrophy) and duration than Aß pathology (Arriagada et al., 1992). With the discovery of high levels of Aß (soluble and insoluble) in preternaturally long-lived NMRs (Edrey et al., 2013), we focused on the role of tau protein in their innate resistance to Aß neurotoxicity. Our comparison of putative NMR tau protein, derived from the sequenced NMR genome (Kim et al., 2011), with human tau protein indicated 95% sequence identity (Fig. 1). In agreement to the *in silico* prediction, we found that NMR brain homogenates contained protein highly immunoreactive to eight distinct anti-human tau antibodies. Although neonatal NMR tau appears similar in size to human tau, a progressive increase in NMR tau molecular weight occurs throughout development resulting in an adult-expressed 88 kDa protein remarkably larger than tau protein reported from other species (Fig. 2). We found that NMR tau is phosphorylated at several epitopes throughout life. Although the highest levels of tau phosphorylation occur during development, even adult NMRs express higher levels of total and phospho-tau than 15-month-old 3xTg-AD mice with overt tau pathology (Fig. 6). Mechanistically, we found tau kinase activity is tightly regulated throughout the NMR life span, indicating a physiological role of tau phosphorylation in these

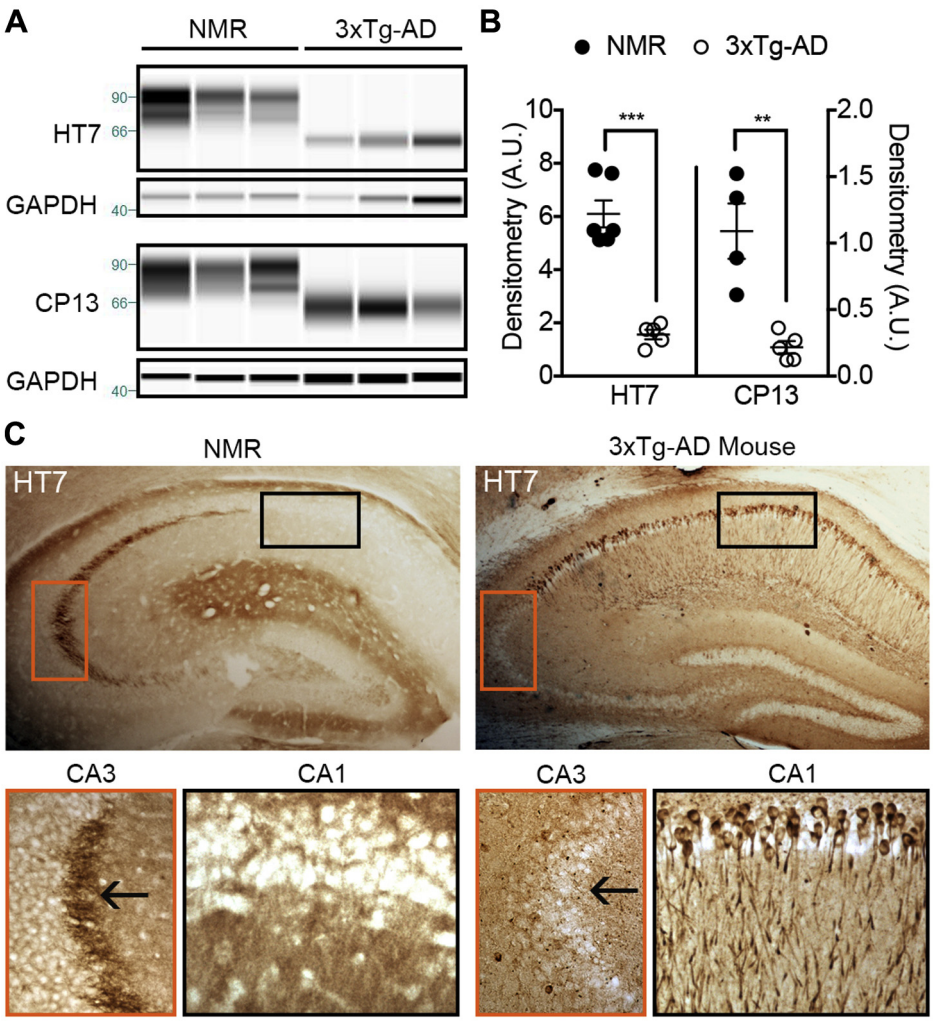

Fig. 6. Adult naked mole-rats (NMRs) express more HT7-tau and phospho-tau than 3xTg-AD mice with overt pathology. (A) Capillary electrophoresis of 7-year-old NMR and 15-month-old 3xTg-AD brain homogenates probed for total tau (HT7) and phospho-Ser^{202}/Thr^{205} tau (CP13). (B) Corresponding densitometry indicates that NMRs express significantly higher HT7 total tau (***: unpaired t test, $p < 0.0001$) and pSer^{202}/Thr^{205} (**: unpaired t test, $p = 0.0025$). (C) IHC with hippocampal tissue from representative NMR and 3xTg-AD mice revealed that NMRs maintain axonal tau expression in the mossy fibers but 3xTg-AD mice do not (CA3 inset, arrow points to mossy fibers). Instead tau from 3xTg-AD mice has inappropriately accumulated in neuronal soma and dendrites (CA1 inset). Abbreviations: AD, Alzheimer's disease; IHC, immunohistochemical. (For interpretation of the references to color in this Figure, the reader is referred to the Web version of this article.)

animals (Figs. 3–6). Despite high levels of total and phospho-tau levels, NMRs appropriately maintain tau expression within the axonal compartment, which contrasts to the mislocalized somato-dendritic tau in 3xTg-AD hippocampal neurons and suggests sustained physiologic, not pathogenic, NMR tau function.

Neurons undergo many ontogenetic phases including proliferation, migration, fate determination, differentiation, formation of axonal pathways, and synaptic connections, all requiring a dynamic cytoskeleton. Tau phosphorylation rapidly alters microtubule stability by decreasing microtubule-binding affinity and helps accommodate dynamic needs of these developing neurons (Biernat et al., 1993; Bramblett et al., 1993; Goedert et al., 1991; Hirokawa, 1994; Lindwall and Cole, 1984). After neurons have completed axonal path-finding, the elaborate and competitive feat to establish appropriate connections, about half of them undergo one final phase of development: degeneration and death (Burek and Oppenheim, 1996; Oppenheim, 1991; Yuan et al., 2003). This counterintuitive, nonpathologic, massive neuronal death requires disassembly of microtubules, which is facilitated by heavy tau phosphorylation (Lindwall and Cole, 1984). Accordingly, tau from prepubescent developing NMR brains is heavily phosphorylated (Fig. 4). Significantly, higher levels of total tau and phospho-tau in the first months of NMR life (Figs. 3 and 4) than adulthood may reflect the overabundance of newly born neurons undergoing axonal migration; the significant decrease through 6 months of age may reflect the final stages of brain development: formation of neural networks and the normal event of massive neuronal death.

Axons of functionally active, mature neurons in the adult nervous system remain static to preserve the neural pathways and established signaling networks. Correspondingly, tau is not heavily phosphorylated in the adult nervous system. Histological and biochemical assessment revealed that NMRs, like other mammals (Kenessey and Yen, 1993), express less phosphorylated tau in adulthood than in development (Fig. 4). Unlike other rodents, however, NMRs displayed high levels of phospho-tau longer throughout development, between three and six months of age, than the three weeks observed in mice and rats. This prolonged period of high phospho-tau may reflect the NMR extended developmental period. Although mice and rats reach sexual maturity 4–6 weeks of age, NMRs prepubescent period extends through the first six months of life. Recent studies suggest that delayed NMR maturation pertains not only to their reproductive system but also includes brain development as well as the

maintenance of several neotenous traits even into adulthood (Buffenstein, 2001; Peterson et al., 2012a,b,). For example, while investigating hypoxia tolerance, a feature common to neonatal brains, NMRs were found to maintain this feature weeks longer than mice (Peterson et al., 2012a). Compared with hippocampal slices cultured from mice that display an adult-like response to hypoxia by postnatal day 20, NMRs calcium response remains blunted through postnatal day 42. Although NMR hypoxia response was abnormal compared with mice at all ages tested, a significant age-related increase occurred between postnatal days 6–20 (Peterson et al., 2012a), which coincides with the first major change in tau protein size reported here (Fig. 2). To cope with low oxygen availability *in utero*, developing mammalian neonates express an NMDA subunit that is less hypoxia sensitive than adult NMDA receptors, and NMRs retain expression of this neonatal subunit, NRD2, longer than mice (Bickler et al., 2003). In a separate study stabilizing microfilaments with phalloidin prevented the hypoxia-induced decrease in NMDA receptor function in postnatal day 3–10 rat neurons (Bickler et al., 2003). This finding not only emphasizes the importance of cytoskeletal stability during hypoxia, possibly for receptor internalization, but also suggests that the tau molecular weight shifts observed here correspond with neuronal maturation milestones in NMR development. The delayed brain development in NMRs may contribute to their extreme longevity, as short-lived animals often are born precocious or with accelerated sexual maturation.

Phosphorylation dramatically alters tau molecular weight. For example, recombinant 4R2N human tau protein has a molecular weight of 45.9 kDa, whereas the heavily phosphorylated pathogenic tau protein extracted from AD patient brains is 72 and/or 74 kDa (for reviews see Ozansoy and Baska, 2007). To assess the contribution of phosphorylation on the developmental increase in tau molecular weight, we probed brain homogenates with antibodies specific to tau phosphorylation before and after the addition of phosphatase (Fig. 4). NMR tau was immunoreactive to tau phosphorylated at $Ser^{396/404}$, and phosphatase treatment greatly reduced the molecular weight indicating that NMR tau is heavily phosphorylated in development and adulthood (Fig. 4). However, even phosphatase-treated samples displayed an age-dependent difference in molecular weight suggesting that other post-translational modifications may contribute, in part, to the difference in molecular weight (Martin et al., 2011). Another possibility is that NMRs incorporate unique exons through alternative splicing that other mammals do not naturally express. Because our assessment of NMR sequence data indicates that NMR *Mapt* brain transcript is similar in length to that of humans (Kim et al., 2011; http://naked-mole-rat.org/), we are exploring tau alternative splicing during development and aging in our ongoing studies.

Kinase dysregulation has catastrophic implications in myriad signaling cascades. In regard to tau metabolism, kinase hyperactivity resulting in tau hyperphosphorylation can cause its misfolding, aggregation, decreased solubility, and eventual neurodegeneration and dementia in various tauopathies including AD (for reviews see Cruz and Tsai, 2004; Leroy et al., 2007; Martin et al., 2013; Vogelsberg-Ragaglia et al., 2001; Wang et al., 2007). We have not seen overt brain pathology even in NMRs >20 years old, suggesting precise regulatory control of kinases throughout the extraordinarily long NMR life span (Edrey et al., 2013). Here, we found stable levels of Cdk5, p35, and ERK2. Furthermore, increased inhibitory GSK3ß phosphorylation at Ser^{9} during development is indicative of regulated activity during this potentially vulnerable period marked by high levels of total GSK3ß (Fig. 5). In the oldest cohort we did, however, find increased levels of ERK2 phosphorylated at activation loop residues $Thr^{185/187}$ (Fig. 5). It is tempting to speculate that high levels of phospho-ERK2 relate to successful healthy brain aging as this 30-year-old cohort is comparable with supercentenarian humans. Alternately, it may reflect their social status as the colony's eldest members. Indeed, ERK2 activity has been shown to play a crucial role in social, cognitive, and social behavior in mice (Satoh et al., 2011). Additional studies comparing ERK2 phosphorylation between animals of different social hierarchy will help elucidate this possibility.

Previously, we compared Aß expression levels between NMRs and 3xTg-AD mice. Surprisingly, we found that NMRs expressed higher levels of Aß than the genetically engineered AD mouse model (Edrey et al., 2013). In our present study, we found that NMRs also express higher levels of total and phospho-tau than 3xTg-AD mice (Fig. 6). Although NMR brains contain elevated levels of both AD-associated proteins (Aß and phospho-tau) they do not develop manifest Aß plaques, neurofibrillary tangle pathology, or neuronal loss even in the oldest cohort (30-year-old NMRs). Furthermore, unlike 3xTg-AD hippocampal neurons displaying hyperphosphorylated tau mislocalized to the somatodendritic compartment NMRs appropriately maintained axonal tau localization despite appreciable tau phosphorylation (Fig. 6). These data strongly suggest a physiological relevance for the high levels of phospho-tau in life-long brain maintenance and overall neuronal integrity in this unique mammal. Our results represent a paradigm shift suggesting that high levels of both Aß and phospho-tau may indeed be important neural regulators, especially in conditions of high oxidative stress as seen in NMRs (Edrey et al., 2014) rather than simply biomarkers of a diseased state. Supporting this premise, phospho-tau has been shown to protect against oxidative stress (Lee et al., 2005) and neuronal apoptosis (Morsch et al., 1999), and neurons survive decades with tau aggregated neurofibrillary tangles (Li et al., 2007). Elevated levels of Aß and phospho-tau in AD may possibly reflect that protective mechanisms have been overwhelmed as AD takes hold as Aß, too, has shown to be neuroprotective in both developing and mature neurons (Giuffrida et al., 2009) and cerebral interstitial Aß levels positively correlate with neurologic status (Brody et al., 2008).

Because most animal species do not naturally develop measurable levels of brain Aß or phospho-tau, transgenic mice have been the mainstay of AD research. Sporadic and familial AD, although differing in etiology, have similar pathologies suggesting that they may arise through similar pathogenic mechanisms once initiated. This assumption, although key in modeling aspects of AD, has failed to produce translational therapeutics to AD patients. Furthermore, a recent study clearly indicated differences in tau pathology between mutant and wild-type expressed proteins, suggesting distinct pathogenic mechanisms between familial and sporadic disease (Dujardin et al., 2014). Because the vast majority of patients (>98%) do not carry genetic AD mutations, there is a critical need for sporadic animal models to complement the genetic models currently used. Despite high risk factors for developing AD: insulin resistance (Kramer and Buffenstein, 2004) and high levels of brain oxidative stress (Edrey et al., 2014), Aß (Edrey et al., 2013) and phosphorylated tau (Figs 4 and 6), NMRs do not succumb to these toxic insults. Understanding mechanisms used by these remarkable long-lived mammals to curtail neurodegenerative disease will provide great insight into protective mechanisms that may translate to maintained brain function in other species, including humans. In this study, evaluating NMR tau metabolic changes with age, we clearly show that phosphorylated tau is not neurodegenerative, and that the high molecular weight protein offers unique insight into sustained neuronal maintenance.

Disclosure statement

The authors state that they have nothing to disclose and that there are no potential conflicts of interest.

Acknowledgements

The authors thank Yael Edrey, Kelly Grimes, Kaitlyn Lewis, and Karl Rodriguez for help with tissue harvesting and Megan Smith for the care of the animals. This study was approved by the IACUC at UTHSCSA. This work was supported by the American Federation for Aging Research, the Glenn Foundation, and the NIA and/or NIH AG022891. Miranda Orr is supported by a training grant from the National Institute on Aging (T32AG021890).

References

Ahmed, T., Van der Jeugd, A., Blum, D., Galas, M.C., D'Hooge, R., Buee, L., Balschun, D., 2014. Cognition and hippocampal synaptic plasticity in mice with a homozygous tau deletion. Neurobiol. Aging 35, 2474–2478.

Ando, K., Leroy, K., Heraud, C., Yilmaz, Z., Authelet, M., Suain, V., De Decker, R., Brion, J.P., 2011. Accelerated human mutant tau aggregation by knocking out murine tau in a transgenic mouse model. Am. J. Pathol. 178, 803–816.

Andorfer, C., Kress, Y., Espinoza, M., de Silva, R., Tucker, K.L., Barde, Y.A., Duff, K., Davies, P., 2003. Hyperphosphorylation and aggregation of tau in mice expressing normal human tau isoforms. J. Neurochem. 86, 582–590.

Arriagada, P.V., Growdon, J.H., Hedley-Whyte, E.T., Hyman, B.T., 1992. Neurofibrillary tangles but not senile plaques parallel duration and severity of Alzheimer's disease. Neurology 42 (3 Pt 1), 631–639.

Beccano-Kelly, D.A., Kuhlmann, N., Tatarnikov, I., Volta, M., Munsie, L.N., Chou, P., Cao, L.-P., Han, H., Tapia, L., Farrer, M.J., Milnerwood, A.J., 2014. Synaptic function is modulated by LRRK2 and glutamate release is increased in cortical neurons of G2019S LRRK2 knock-in mice. Front. Cell. Neurosci. 8, 301–311.

Bickler, P.E., Fahlman, C.S., Taylor, D.M., 2003. Oxygen sensitivity of NMDA receptors: relationship to NR2 subunit composition and hypoxia tolerance of neonatal neurons. Neuroscience 118, 25–35.

Biernat, J., Gustke, N., Drewes, G., Mandelkow, E.M., Mandelkow, E., 1993. Phosphorylation of Ser262 strongly reduces binding of tau to microtubules: distinction between PHF-like immunoreactivity and microtubule binding. Neuron 11, 153–163.

Bramblett, G.T., Goedert, M., Jakes, R., Merrick, S.E., Trojanowski, J.Q., Lee, V.M., 1993. Abnormal tau phosphorylation at Ser396 in Alzheimer's disease recapitulates development and contributes to reduced microtubule binding. Neuron 10, 1089–1099.

Brion, J.P., Smith, C., Couck, A.M., Gallo, J.M., Anderton, B.H., 1993. Developmental changes in tau phosphorylation: fetal tau is transiently phosphorylated in a manner similar to paired helical filament-tau characteristic of Alzheimer's disease. J. Neurochem. 61, 2071–2080.

Brody, D.L., Magnoni, S., Schwetye, K.E., Spinner, M.L., Esparza, T.J., Stocchetti, N., Zipfel, G.J., Holtzman, D.M., 2008. Amyloid-beta dynamics correlate with neurological status in the injured human brain. Science 321, 1221–1224.

Buffenstein, R., 2001. Ecophysiological responses of subterranean rodents to underground habitats. In: Lacey, E.A., Patton, J.L., Cameron, G.N. (Eds.), Life Underground, the Biology of Subterranean Rodents. University of Chicago Press, Chicago, pp. 62–110.

Burek, M.J., Oppenheim, R.W., 1996. Programmed cell death in the developing nervous system. Brain Pathol. 6, 427–446.

Creamer, J.S., Oborny, N.J., Lunte, S.M., 2014. Recent advances in the analysis of therapeutic proteins by capillary and microchip electrophoresis. Anal. Methods 6, 5427–5449.

Cruz, J.C., Tsai, L.H., 2004. A Jekyll and Hyde kinase: roles for Cdk5 in brain development and disease. Curr. Opin. Neurobiol. 14, 390–394.

Dawson, H.N., Cantillana, V., Jansen, M., Wang, H., Vitek, M.P., Wilcock, D.M., Lynch, J.R., Laskowitz, D.T., 2010. Loss of tau elicits axonal degeneration in a mouse model of Alzheimer's disease. Neuroscience 169, 516–531.

Dujardin, S., Lecolle, K., Caillierez, R., Begard, S., Zommer, N., Lachaud, C., Carrier, S., Dufour, N., Auregan, G., Winderickx, J., Hantraye, P., Deglon, N., Colin, M., Buee, L., 2014. Neuron-to-neuron wild-type tau protein transfer through a trans-synaptic mechanism: relevance to sporadic tauopathies. Acta Neuropathol. Commun. 2, 14.

Edrey, Y.H., Medina, D.X., Gaczynska, M., Osmulski, P.A., Oddo, S., Caccamo, A., Buffenstein, R., 2013. Amyloid beta and the longest-lived rodent: the naked mole-rat as a model for natural protection from Alzheimer's disease. Neurobiol. Aging 34, 2352–2360.

Edrey, Y.H., Oddo, S., Cornelius, C., Caccamo, A., Calabrese, V., Buffenstein, R., 2014. Oxidative damage and amyloid-beta metabolism in brain regions of the longest-lived rodents. J. Neurosci. Res. 92, 195–205.

Giuffrida, M.L., Caraci, F., Pignataro, B., Cataldo, S., De Bona, P., Bruno, V., Molinaro, G., Pappalardo, G., Messina, A., Palmigiano, A., Garozzo, D., Nicoletti, F., Rizzarelli, E., Copani, A., 2009. Beta-amyloid monomers are neuroprotective. J. Neurosci. 29, 10582–10587.

Goedert, M., Crowther, R.A., Garner, C.C., 1991. Molecular characterization of microtubule-associated proteins tau and MAP2. Trends Neurosci. 14, 193–199.

Goedert, M., Spillantini, M.G., Jakes, R., Rutherford, D., Crowther, R.A., 1989a. Multiple isoforms of human microtubule-associated protein tau: sequences and localization in neurofibrillary tangles of Alzheimer's disease. Neuron 3, 519–526.

Goedert, M., Spillantini, M.G., Potier, M.C., Ulrich, J., Crowther, R.A., 1989b. Cloning and sequencing of the cDNA encoding an isoform of microtubule-associated protein tau containing four tandem repeats: differential expression of tau protein mRNAs in human brain. EMBO J. 8, 393–399.

Hardy, J.A., Higgins, G.A., 1992. Alzheimer's disease: the amyloid cascade hypothesis. Science 256, 184–185.

Himmler, A., Drechsel, D., Kirschner, M.W., Martin Jr., D.W., 1989. Tau consists of a set of proteins with repeated C-terminal microtubule-binding domains and variable N-terminal domains. Mol. Cell. Biol. 9, 1381–1388.

Hirokawa, N., 1994. Microtubule organization and dynamics dependent on microtubule-associated proteins. Curr. Opin. Cel. Biol. 6, 74–81.

Kenessey, A., Yen, S.H., 1993. The extent of phosphorylation of fetal tau is comparable to that of PHF-tau from Alzheimer paired helical filaments. Brain Res. 629, 40–46.

Kim, E.B., Fang, X., Fushan, A.A., Huang, Z., Lobanov, A.V., Han, L., Marino, S.M., Sun, X., Turanov, A.A., Yang, P., Yim, S.H., Zhao, X., Kasaikina, M.V., Stoletzki, N., Peng, C., Polak, P., Xiong, Z., Kiezun, A., Zhu, Y., Chen, Y., Kryukov, G.V., Zhang, Q., Peshkin, L., Yang, L., Bronson, R.T., Buffenstein, R., Wang, B., Han, C., Li, Q., Chen, L., Zhao, W., Sunyaev, S.R., Park, T.J., Zhang, G., Wang, J., Gladyshev, V.N., 2011. Genome sequencing reveals insights into physiology and longevity of the naked mole rat. Nature 479, 223–227.

Kramer, B., Buffenstein, R., 2004. The pancreas of the naked mole-rat (Heterocephalus glaber): an ultrastructural and immunocytochemical study of the endocrine component of thermoneutral and cold acclimated animals. Gen. Comp. Endocrinol. 139, 206–214.

Lee, H.G., Perry, G., Moreira, P.I., Garrett, M.R., Liu, Q., Zhu, X., Takeda, A., Nunomura, A., Smith, M.A., 2005. Tau phosphorylation in Alzheimer's disease: pathogen or protector? Trends Mol. Med. 11, 164–169.

Lei, P., Ayton, S., Finkelstein, D.I., Spoerri, L., Ciccotosto, G.D., Wright, D.K., Wong, B.X., Adlard, P.A., Cherny, R.A., Lam, L.Q., Roberts, B.R., Volitakis, I., Egan, G.F., McLean, C.A., Cappai, R., Duce, J.A., Bush, A.I., 2012. Tau deficiency induces parkinsonism with dementia by impairing APP-mediated iron export. Nat. Med. 18, 291–295.

Leroy, K., Yilmaz, Z., Brion, J.P., 2007. Increased level of active GSK-3beta in Alzheimer's disease and accumulation in argyrophilic grains and in neurones at different stages of neurofibrillary degeneration. Neuropathol. Appl. Neurobiol. 33, 43–55.

Li, H.L., Wang, H.H., Liu, S.J., Deng, Y.Q., Zhang, Y.J., Tian, Q., Wang, X.C., Chen, X.Q., Yang, Y., Zhang, J.Y., Wang, Q., Xu, H., Liao, F.F., Wang, J.Z., 2007. Phosphorylation of tau antagonizes apoptosis by stabilizing beta-catenin, a mechanism involved in Alzheimer's neurodegeneration. Proc. Natl. Acad. Sci. U. S. A. 104, 3591–3596.

Lindwall, G., Cole, R.D., 1984. Phosphorylation affects the ability of tau protein to promote microtubule assembly. J. Biol. Chem. 259, 5301–5305.

Martin, L., Latypova, X., Terro, F., 2011. Post-translational modifications of tau protein: implications for Alzheimer's disease. Neurochem. Int. 58, 458–471.

Martin, L., Latypova, X., Wilson, C.M., Magnaudeix, A., Perrin, M.L., Yardin, C., Terro, F., 2013. Tau protein kinases: involvement in Alzheimer's disease. Ageing Res. Rev. 12, 289–309.

Morsch, R., Simon, W., Coleman, P.D., 1999. Neurons may live for decades with neurofibrillary tangles. J. Neuropathol. Exp. Neurol. 58, 188–197.

Nguyen, U., Squaglia, N., Boge, A., Fung, P.A., 2011. The Simple Western: a gel-free, blot-free, hands-free Western blotting reinvention. Nat. Methods 8, v–vi.

Oddo, S., Caccamo, A., Shepherd, J.D., Murphy, M.P., Golde, T.E., Kayed, R., Metherate, R., Mattson, M.P., Akbari, Y., LaFerla, F.M., 2003. Triple-transgenic model of Alzheimer's disease with plaques and tangles: intracellular Abeta and synaptic dysfunction. Neuron 39, 409–421.

Oppenheim, R.W., 1991. Cell death during development of the nervous system. Annu. Rev. Neurosci. 14, 453–501.

Ozansoy, M.B., Baska, A.N., 2007. Tauopathies: a distinct class of neurodegenerative diseases. BJMG 10, 3–14.

Pacheco, C.D., Elrick, M.J., Lieberman, A.P., 2009. Tau deletion exacerbates the phenotype of Niemann-Pick type C mice and implicates autophagy in pathogenesis. Hum. Mol. Genet. 18, 956–965.

Peterson, B.L., Larson, J., Buffenstein, R., Park, T.J., Fall, C.P., 2012a. Blunted neuronal calcium response to hypoxia in naked mole-rat hippocampus. PLoS One 7, e31568.

Peterson, B.L., Park, T.J., Larson, J., 2012b. Adult naked mole-rat brain retains the NMDA receptor subunit GluN2D associated with hypoxia tolerance in neonatal mammals. Neurosci. Lett. 506, 342–345.

Rovelet-Lecrux, A., Campion, D., 2012. Copy number variations involving the microtubule-associated protein tau in human diseases. Biochem. Soc. Trans. 40, 672–676.

Satoh, Y., Endo, S., Nakata, T., Kobayashi, Y., Yamada, K., Ikeda, T., Takeuchi, A., Hiramoto, T., Watanabe, Y., Kazama, T., 2011. ERK2 contributes to the control of social behaviors in mice. J. Neurosci. 31, 11953–11967.

Spillantini, M.G., Goedert, M., 2013. Tau pathology and neurodegeneration. Lancet Neurol. 12, 609–622.

Vogelsberg-Ragaglia, V., Schuck, T., Trojanowski, J.Q., Lee, V.M., 2001. PP2A mRNA expression is quantitatively decreased in Alzheimer's disease hippocampus. Exp. Neurol. 168, 402–412.

Wang, J.Z., Grundke-Iqbal, I., Iqbal, K., 2007. Kinases and phosphatases and tau sites involved in Alzheimer neurofibrillary degeneration. Eur. J. Neurosci. 25, 59–68.

Wirths, O., Bayer, T.A., 2010. Neuron loss in transgenic mouse models of Alzheimer's disease. Int. J. Alzheimers Dis. 2010. http://dx.doi.org/10.4061/2010/723782; pii: 723782.

Yuan, J., Lipinski, M., Degterev, A., 2003. Diversity in the mechanisms of neuronal cell death. Neuron 40, 401–413.

Zahs, K.R., Ashe, K.H., 2010. 'Too much good news' - are Alzheimer mouse models trying to tell us how to prevent, not cure, Alzheimer's disease? Trends Neurosci. 33, 381–389.